



Etiology and epidemiology of Botryosphaeria canker of *Eucalyptus urophylla* S. T. Blake in pure stand and an integrated crop-livestock-forest system

Etiologia e epidemiologia do cancro de Botryosphaeria em *Eucalyptus urophylla* S. T. Blake em povoamento puro e sistema integrado lavoura-pecuária-floresta

Etiología y epidemiología del cancro de Botryosphaeria de *Eucalyptus urophylla* S. T. Blake en rodal puro y en un sistema integrado cultivo-ganado-bosque

DOI: 10.55905/revconv.18n.3-082

Originals received: 2/10/2025

Acceptance for publication: 3/4/2025

Aline Pereira Gomes

Master's in Forest Engineering

Institution: Universidade Federal do Acre (UFAC)

Address: Rio Branco – Acre, Brazil

E-mail: alinecesp.2017@gmail.com

Nei Sebastião Braga Gomes

Ph.D. in Forest Engineering

Institution: Universidade Federal do Acre (UFAC)

Address: Rio Branco – Acre, Brazil

E-mail: nei.gomes@ufac.br

Rivaldalve Coelho Gonçalves

Ph.D. in Agronomy

Institution: Empresa Brasileira de Pesquisa Agropecuária (EMBRAPA)

Address: Rio Branco – Acre, Brazil

E-mail: rivadalvegoncalves@embrapa.br

Celso Garcia Auer

Ph.D. in Agronomy

Institution: Empresa Brasileira de Pesquisa Agropecuária (EMBRAPA)

Address: Colombo – Paraná, Brazil

E-mail: celso.auer@embrapa.br

Waldir Cintra de Jesus Junior

Ph.D. in Phytopathology

Institution: Universidade Federal de São Carlos (UFSCAR)

Address: São Carlos – São Paulo, Brazil

E-mail: wcintra@ufscar.br



Lucas Gracioli Savian

Ph.D. in Forest Engineering

Institution: Universidade Federal do Acre (UFAC)

Address: Rio Branco – Acre, Brazil

E-mail: lucassavian17@gmail.com

ABSTRACT

Diseases in *Eucalyptus* plants can reduce forestry production. This study aimed to identify the causal agents of cankers in *Eucalyptus urophylla* trees in two systems: a pure stand system (PSS) and an integrated crop-livestock-forest system (ICLFS) with *Urochloa brizantha*. Diseased trees were sampled from trunks, stems, and branches for fungal isolation. Data were collected from two plots per system (500 trees/plot) to analyze disease dynamics, structure, and spatial distribution in the plots and along row directions. Isolates were identified morphologically as *Lasiodiplodia* spp., *Pestalotiopsis* spp., and *Coniella* spp. Phylogenetic analysis of the TEF1- α sequence identified *Lasiodiplodia* spp. AR2P28 as *Lasiodiplodia theobromae* and *Pestalotiopsis* spp. AR1P22 as *Neopestalotiopsis surinamensis*. Analysis of the ITS sequence identified *Lasiodiplodia* spp. AR4P15 as *Lasiodiplodia citricola*. In areas 1, 3, and 4, the disease showed an aggregated spatial pattern, except in P2 of area 1 with a 3x2 quadrat. Area 2 had a random spatial pattern in both quadrat sizes, except for P1 in the 3x2 quadrat. Regarding row direction, areas 1 and 2 had a random pattern, while areas 3 and 4 had an aggregated pattern. The disease had a higher incidence in the ICLFS compared to the PSS, with an increase of 23.6% to 155%. Disease incidence ranged from 34.2% to 87.2%, with fewer foci, mainly compact, and a high number of diseased plants per focus, particularly in areas 3 and 4 in the ICLFS.

Keywords: tree-diseases, tree-fungi, diagnosis, *Coniella*, *Lasiodiplodia*, *Neopestalotiopsis*.

RESUMO

As doenças nas plantas de eucalipto podem reduzir a produção florestal. O objetivo deste estudo foi identificar os agentes causadores dos cancrios em árvores de *Eucalyptus urophylla* em dois sistemas: o sistema de plantio puro (PSS) e o sistema integrado de lavoura-pecuária-floresta (ICLFS) com *Urochloa brizantha*. Árvores doentes foram amostradas nos troncos, caules e galhos para isolamento de fungos. A coleta de dados foi realizada em duas parcelas por sistema (500 árvores/parcelas) para analisar a dinâmica da doença, a estrutura e a distribuição espacial nas parcelas e na direção das fileiras. Os isolados foram identificados morfologicamente como *Lasiodiplodia* spp., *Pestalotiopsis* spp. e *Coniella* spp. A análise filogenética da sequência TEF1- α identificou *Lasiodiplodia* spp. AR2P28 como *Lasiodiplodia theobromae* e *Pestalotiopsis* spp. AR1P22 como *Neopestalotiopsis surinamensis*. A análise da sequência ITS identificou *Lasiodiplodia* spp. AR4P15 como *Lasiodiplodia citricola*. Nas áreas 1, 3 e 4, a doença apresentou um padrão espacial agregado, exceto na P2 da área 1 com quadrat de 3x2. A área 2 apresentou um padrão espacial aleatório em ambos os tamanhos de quadrat, exceto na P1 com quadrat 3x2. Na direção das fileiras, as áreas 1 e 2 apresentaram um padrão aleatório, enquanto as áreas 3 e 4 apresentaram um padrão agregado. A doença teve maior incidência no ICLFS em comparação ao PSS, com aumento de 23,6% a 155%. A incidência variou de 34,2% a 87,2%, com menor número de focos, principalmente compactos, e maior número de plantas doentes por foco, especialmente nas áreas 3 e 4 do ICLFS.



Palavras-chave: doenças de árvores, fungos de árvores, diagnóstico espacial, *Coniella*, *Lasiodiplodia*, *Neopestalotiopsis*.

RESUMEN

Las enfermedades en las plantas de eucalipto pueden reducir la producción forestal. El objetivo de este estudio fue identificar los agentes causantes de los canchros en árboles de *Eucalyptus urophylla* en dos sistemas: el sistema de plantación pura (PSS) y el sistema integrado de agricultura-ganadería-forestal (ICLFS) con *Urochloa brizantha*. Se tomaron muestras de árboles enfermos en troncos, tallos y ramas para el aislamiento de hongos. La recolección de datos se realizó en dos parcelas por sistema (500 árboles/parcelas) para analizar la dinámica de la enfermedad, la estructura y la distribución espacial en las parcelas y en la dirección de las filas. Los aislados se identificaron morfológicamente como *Lasiodiplodia* spp., *Pestalotiopsis* spp. y *Coniella* spp. El análisis filogenético de la secuencia TEF1- α identificó *Lasiodiplodia* spp. AR2P28 como *Lasiodiplodia theobromae* y *Pestalotiopsis* sp. AR1P22 como *Neopestalotiopsis surinamensis*. El análisis de la secuencia ITS identificó *Lasiodiplodia* spp. AR4P15 como *Lasiodiplodia citricola*. En las áreas 1, 3 y 4, la enfermedad mostró un patrón espacial agregado, excepto en P2 del área 1 con un cuadrado de 3x2. El área 2 mostró un patrón espacial aleatorio en ambos tamaños de cuadrícula, excepto en P1 con cuadrado 3x2. En la dirección de las filas, las áreas 1 y 2 mostraron un patrón aleatorio, mientras que las áreas 3 y 4 mostraron un patrón agregado. La enfermedad tuvo una mayor incidencia en el ICLFS en comparación con el PSS, con un aumento del 23,6% al 155%. La incidencia varió del 34,2% al 87,2%, con menos focos, principalmente compactos, y un mayor número de plantas enfermas por foco, especialmente en las áreas 3 y 4 del ICLFS.

Palabras clave: enfermedades de árboles, hongos de árboles, diagnóstico, *Coniella*, *Lasiodiplodia*, *Neopestalotiopsis*.

1 INTRODUCTION

The forestry of even-aged *Eucalyptus* forest in Brazil is highly developed. countries. *Eucalyptus* forests are cultivated to produce paper, pulp, energy, charcoal, wood for furniture, rural structures, fences, buildings, oils, and ecological externalities. These forests produce paper, pulp, energy, charcoal, wood, oils, and ecological benefits. In 2019, planted forests covered approximately 9 million hectares, with *Eucalyptus* accounting for 6.9 million hectares and generating R\$ 97.4 billion and share of 1.2% of the national GDP (IBA, 2020). Native to Australia, *Eucalyptus* has increasingly faced pest and disease issues (Alfenas *et al.*, 2004; Wingfield *et al.*, 2008), with *Eucalyptus* canker caused by *Chrysosporthe cubensis* being historically significant. Other cankers, such as those caused by *Botryosphaeria* spp., exhibit similar symptoms (Alfenas *et al.*, 2004).



For the anamorph *Lasiodiplodia theobromae*, reports exist of the teleomorph *Botryosphaeria rhodina* (syn. *Botryodiplodia theobromae*) (Roux *et al.*, 2001) and *B. ribis* (Alfenas *et al.*, 2004). However, *L. theobromae* was established as a single valid name for both asexual and sexual phases, with no proven connection to a sexual taxon (Phillips *et al.*, 2013).

In Acre, small forests of *Eucalyptus urophylla* and *E. urophylla* × *E. grandis* are commercially planted in pure stands and integrated crop-livestock-forest systems (ICLFS). Some trees exhibited severe disease symptoms, including cankers, dieback, loss of apical dominance, and kino exudation, affecting growth. These symptoms, combined with a favorable environment, supported the hypothesis of *Botryosphaeria* canker in *E. urophylla*, with differences in incidence, spatial pattern, and disease dynamics among stand types. This study aimed to identify the causal fungi, assess disease intensity, and analyze spatial patterns and focus structures in both pure stands and ICLFS in the Vale do Acre mesoregion, Brazil.

2 MATERIAL AND METHODS

2.1 STUDY SITE

The evaluations and collection of diseased plants for fungal isolation were conducted in four non-contiguous areas in the municipalities: Rio Branco, Senador Guiomard, and Porto Acre, in the Mesoregion Vale do Acre, between May and June 2019. *Eucalyptus urophylla*, clone I144, plantations were established between 2015 and 2017.

Areas 1 and 2 followed a conventional planting system (pure stand system, PSS, 3.3 m × 2.8 m), while areas 3 and 4 adopted an integrated crop-livestock-forest system (ICLFS) with *Eucalyptus urophylla*, clone I144, and *Urochloa brizantha*, spaced at 3.0 m × 2.0 m × 35 m, in quadruple (area 3) and double rows (area 4) Each area was divided into two plots of 500 trees, with the total number of trees calculated by multiplying the number of quadrats by the number of plants per quadrat.



2.2 SAMPLE COLLECTION, ISOLATION, AND FUNGI PURIFICATION

Bark tissue and stem wood segments were collected from the trunk or stem, presenting typical cankers, defined as lesions surrounded by callus, in elevated positions of trees with or without signs of apical dominance loss. Samples from 10 randomly selected trees per plot were placed in clean paper bags and transported to the Phytopathology Laboratory of the Federal University of Acre for fungal isolation.

Fungal isolation followed the indirect method (Alfenas *et al.*, 2007). In the laboratory, samples were disinfected in 70% ethanol for 30 s. Fragments (~5 mm × 5 mm) were immersed in 50 mL of sodium hypochlorite (NaClO) at 1,250 ppm for 2 min, then rinsed twice in sterile distilled water. Excess NaClO was removed, and fragments were dried on sterilized filter paper. Four fragments were deposited on PDA (Potato Dextrose Agar) medium supplemented with 50 ppm chloramphenicol in Petri dishes (90 mm × 15 mm). Plates were incubated in a BOD chamber at 25°C for three to four days.

A hyphal fragment from each fungal colony was transferred to the center of sterile plastic Petri dishes containing PDA with 50 ppm chloramphenicol in a vertical laminar flow chamber sterilized with 254 nm UV light, using a flamed needle for pure culture isolation. After confirming colony purity by visual inspection, fungi were transferred to test tubes (150 × 16 mm) with PDA (without antibiotics) and sealed with a cotton plug for temporary preservation.

2.3 FUNGI CHARACTERIZATION AND IDENTIFICATION

Macromorphological characterization of fungal was carried on PDA medium by inspection with the naked eye, and the micromorphological characterization through observations under a light microscope. For *Lasiodiplodia* stains, a 2% agar-water medium with pieces of the stem (ca. 10 mm × 3 mm) from seedlings of *Pinus taeda* L. with approximately 60 days of age was used to induce sporulation.

Putative species of *Lasiodiplodia* (AR2P28, AR3P13, AR3P21, AR4P15, and AR4P23) (Philips *et al.*, 2013) were analyzed using the Jaccard dissimilarity index (DSJ), calculated as $DSJ = 2B / (1 + B)$, where B represents the Bray-Curtis dissimilarity index in its binary form ($B = (A + B - 2*J) / (A + B)$). A distance matrix was constructed, followed by cluster analysis using



UPGMA (Sokal & Michener, 1958) in the R program (v. 3.6.1, Vegan package 2.5-6, and *vegdist* function; Oksanen *et al.*, 2019). The criteria for identifying the isolates at the species level were arbitrarily set to $DSJ = 0$ as evidence of zero dissimilarity of a single species in the distance matrix. The same method was used to identify the strains of putative *Pestalotiopsis* spp. (strains AR1P17, AR1P22, AR2P14, AR2P29, AR3P15, AR3P25, AR4P19, and AR4P21), comparing 20 *Pestalotiopsis* species and four *Neopestalotiopsis* species. Strains of putative *Coniella* spp. (strains AR3P10, AR3P28, AR4P24, and AR4P29) were analyzed with four species of *Harknessia* Cooke, 1881, two species of *Coniella* Von Höhnelt 1918, and seven species of *Pilidiella* Petrak & Sydow 1927.

For the molecular characterization of isolates, monosporic colonies were cultivated on solid PDA and liquid PD (potato dextrose) medium. DNA extraction was carried out according to Doyle and Doyle (1987), using 100 mg of colony mycelium. The extracted DNA was subjected to PCR amplification of the translation elongation factor 1-alpha gene (*tef1*) from the *TEF1- α* genomic region with the oligonucleotide pair EF1-688F and EF1-986R (Alves *et al.*, 2008; Carbone and Khon, 1999).

PCR reactions were performed in tubes containing 5 μ L of 10X buffer, 1 μ L of dNTPs at 2.5 mM, 2.5 μ L of Magnesium Chloride ($MgCl_2$) at 50 mM (final concentration: 2.5 mM), 1 μ L of taq polymerase, 1 μ L of each oligonucleotide (final concentration: 10 pmoles), and 4 μ L of genomic DNA (5 ng/ μ L), along with 7.5 μ L of sterile water. A tube with reagents and water, without DNA, was used as a negative control. The PCR reactions were performed in an Applied Biosystems Veriti 96-well thermal cycler. The conditions for the oligonucleotide primers EF1-688F and EF1-986R were: step 1: denaturation at 95 °C for 5 min; step 2: 35 cycles of 94 °C for 60 s (denaturation), 55 °C for 60 s (annealing), 72 °C for 120 s (elongation); step 3: final extension at 72°C for 10 min.

For the amplification of the ITS region of rDNA, oligonucleotides ITS1-ITS4 and ITS5-ITS4 (White *et al.*, 1990) were used. PCR for both pairs was performed with the following program: step 1: denaturation at 95°C for 5 min; step 2: 35 cycles of 94°C for 60 s (denaturation), 52°C for 60 s (annealing), 72°C for 120 s (elongation); step 3: final extension at 72°C for 10 min.

After PCR cycles, the final contents of the tubes were applied to a 1% agarose gel in 1X TBE, subjected to electrophoresis at 100 volts for 60 min with a 1Kb DNA ladder. The gel was stained with GelRed® and visualized under ultraviolet light (UV-B, 302-312 nm), photographed



using the L-Pix EX image capture system with a 12.4MP CCD camera and Lab Image 1D L320 software.

The sequencing of the PCR products was performed at the Multiuser Laboratory of Genotyping and Sequencing at the State University of Campinas using the same pair of oligonucleotides, the BigDye™ Terminator Cycle Sequencing Kit, and the Genetic Analyzer 3500XL system. The electropherogram files were visualized, edited, and analyzed using BioEdit v7.0 (Hall, 1999).

DNA sequences were aligned using CLUSTAL W within Mega v10.0 (Kumar *et al.*, 2018). Gaps were treated as missing data for further analysis. The ITS and TEF1- α sequences of *Lasiodiplodia* spp. strains AR2P28 and AR4P15 were compared with sequences from fungi of *Diplodia*, *Fusicoccum*, *Lasiodiplodia*, and *Neofusicoccum*. Sequences of *Pestalotiopsis* spp. strain AR1P22 were compared with sequences from fungi in the genera *Pestalotiopsis* and *Neopestalotiopsis*. Phylogenetic trees were constructed using Bayesian Inference (BI) with MrBayes v.3.1.2 (Ronquist & Heulsenbeck, 2003). The tree analysis was performed with 1 million generations, sampling 1 tree for every ten produced, totaling 100,000 trees. The first 25,000 trees were discarded. The final phylogenetic tree was visualized and edited in FigTree 1.3.1 (Rambaut, 2009).

The spatial dispersion pattern of the disease was analyzed in experimental plots across four study areas, totaling two plots of 500 trees each. Diseased plants exhibited typical canker symptoms on the middle and upper thirds of the trees, while healthy plants showed no canker symptoms. Epidemiological analyses were based on binary data (presence or absence of disease in each tree). Sampling units were divided into quadrats, with two sizes tested (4 plants in 2x2 layout and 6 plants in 3x2 layout) to determine the dispersion index (DI). The tree was the spatial unit, and the total number of diseased plants per square was counted to calculate mean incidence using the formula $p = \sum X_i / nN$, where $\sum X_i$ is the total number of diseased trees and nN is the total number of trees in the plot. The dispersion pattern was analyzed using independent observations, binomial distribution, and DI data.

The Dispersion Index used was the Vobs/Vbin ratio, where Vbin represents the binomial variance (Bergamin Filho *et al.*, 2004), calculated as $V_{bin} = (p(1-p))/n$, with p being the mean disease incidence, $(1-p)$ the proportion of healthy plants, and n the number of trees per quadrat. Vobs was calculated as $\sum (X_i - n.p)^2 / n^2(N-1)$, where $\sum X_i$ is the total number of diseased trees in



quadrat i , N is the total number of quadrats, and n and p are defined for V_{bin} (Bergamin Filho *et al.*, 2004). The hypothesis H_0 of a random spatial pattern ($DI \chi^2 = 1$) was tested using the chi-square test (χ^2), at 5% probability (0.05: critical region), with $df = N-1$ degrees of freedom, using the observed value of $\chi^2_{obs(c)}$, calculated as $\chi^2 = DI(N-1)$ (Elliott, 1993). H_0 was accepted if $\chi^2_{obs(c)} \leq \chi^2_{tab}(1-\alpha, df)$, and rejected if $\chi^2_{obs(c)} > \chi^2_{tab}(1-\alpha, df)$. For $N > 31$, the d statistic was calculated as $d = \text{root}(2\chi^2_{obs(c)}) - \text{root}(2df-1)$, and H_0 was considered accepted if $|d| < 1.96$ and rejected if $|d| \geq 1.96$ (Elliott, 1993). The value of $\chi^2_{obs(c)}$ was also tested at 5% probability ($P > 0.05$) with the chi-square statistic calculated by $\chi^2_{calc} = 0.5*[1.645 + (2*(N-1)-1)^{1/2}]^2$, considering χ^2_{calc} as the critical chi-square value and 1.645 as the square root of the critical point 2.706 ($df = 1$, p -value = 0.10) for the one-tailed test. If $\chi^2_{obs(c)} \leq \chi^2_{calc}$, H_0 was accepted, indicating that the data fit the Poisson series and the disease population has a random spatial dispersion pattern. If $\chi^2_{obs(c)} > \chi^2_{calc}$, H_0 was rejected, and the spatial dispersion pattern of the disease population was not random.

According to Bergamin Filho *et al.* (2004), run and doublet analyses were used to understand the disease's spatial dispersion pattern in the planting lines. For the run analysis, the number of runs was defined as a sequence of identical symbols, with diseased plants (+) and healthy plants (-). The expected number of runs $E(R) = 1 + (2m(N-m)/N)$, and variance $\sigma^2(R) = 2m(N-m)[2m(N-m) - N] / [N^2(N-1)]$. The standardized value $ZR = (R + 0.5 - E(R)) / \sigma(R)$ was calculated.

For the doublet analysis, each doublet was formed by two adjacent diseased (+) or healthy plants (-) and counted as 1. The total number of doublets (D) was obtained by summing the observed individual doublets in each planting row. The expected number of doublets $E(D) = m(m-1) / N$, and variance $\sigma^2(D) = [m(m-1) [N(N-1) + 2N(m-2) + N(m-2)(m-3) - (N-1)m(m-1)]] / N^2(N-1)$. A standardized value was calculated as $ZD = [(D + 0.5 - E(D)) / \sigma(D)$ (Bergamin Filho *et al.*, 2004).

The analysis of the dynamics and structure of foci (ADSF) was carried out according to Nelson (1996) and Bergamin Filho *et al.* (2004), considering diseased plants with symptoms in adjacent two-dimensional proximity as foci. In each plot, the number of diseased plants (NDP), maximum number of rows (l_r) and columns (l_c) per focus, number of plants per focus (NPF), unitary and non-unitary focus (NF), unitary focus (NUF), and average number of plants per focus (ANPF) were evaluated. The indices of foci form (IFF), non-unitary foci form (IFNUF), foci



compaction (ICF), and non-unitary foci compaction (ICNUF) were calculated using the formulas: $IFF = \sum 1^n(lfi/lci) / NF$ and $ICF = \sum 1^n[NPFi / (lci * lfi)] / NF$. For IFNUF or ICNUF, non-unitary foci were exclusively considered (Jesus Junior & Bassanezi, 2004). IFF or IFNUF = 1.0 indicates isodiametric foci, IFF or IFNUF > 1.0 indicate longer foci in the planting rows, and IFF or IFNUF < 1.0 reveal longer foci in the planting line direction. ICF or ICNUF values close to 1.0 indicate more compact foci, indicating greater aggregation and proximity between plants (Jesus Junior & Bassanezi, 2004). Pearson's linear correlation was calculated using data from all plots in Rbio software (Bhering, 2017) to test the hypothesis of a linear relationship between disease incidence (I) and total number of foci (NF).

3 RESULTS AND DISCUSSION

3.1 CHARACTERIZATION OF DISEASE SYMPTOMS

In the four study areas, diseased and possibly recovered trees exhibited long-lined cankers in high positions on the trunk, stem, branches, and shoots of different-sized trees, along with die-back, bifurcation of the stem and trunk, trunk tortuosity, dwarfism, and the presence of dry kino impregnated in the bark from the lesions (Figure 1-A, B, and C). These symptoms are identical to those described in the literature exclusively for *Botryosphaeria* Canker (Ferreira & Milani, 2002; Alfenas *et al.*, 2004).

Figure 1. *Eucalyptus urophylla* trunk after sample collection with canker symptoms.



Source: The authors, 2021.

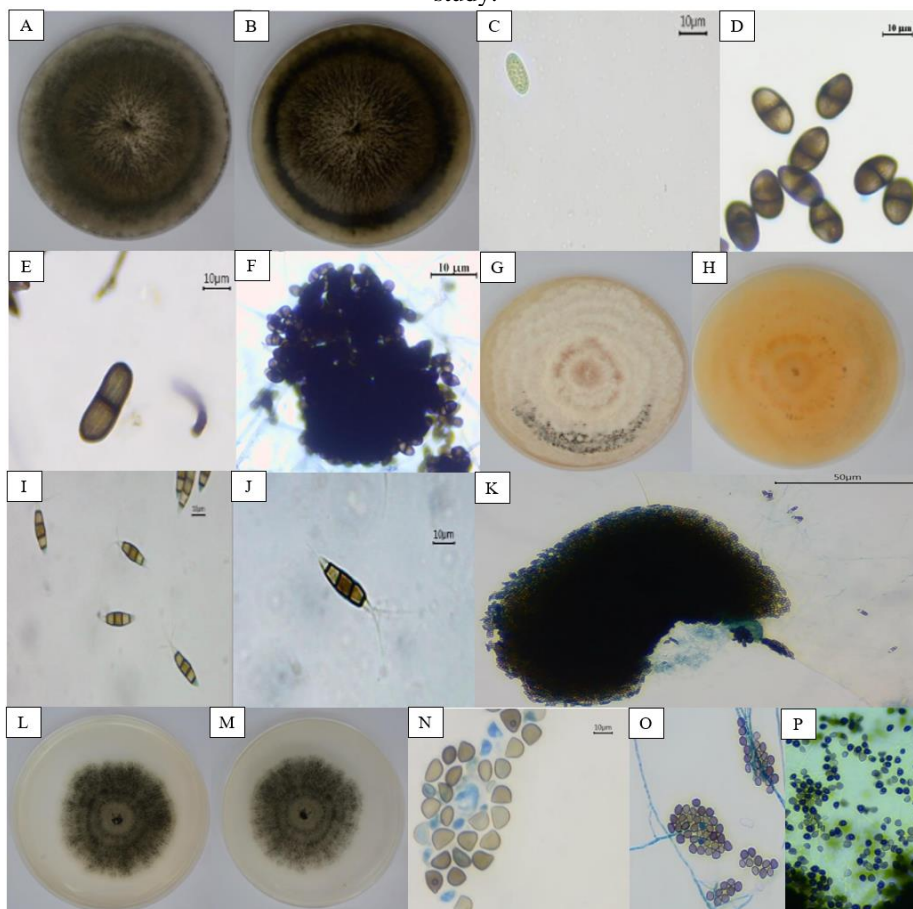


3.2 FUNGI CHARACTERIZATION AND IDENTIFICATION

The fungi isolated from diseased plants were identified based on macroscopic and micromorphological characteristics of three genera: *Lasiodiplodia* spp. (5 isolates), *Pestalotiopsis* spp. (8 isolates), and *Coniella* spp. (4 isolates), totaling 17 isolates. Two isolates of *Lasiodiplodia* spp. (AR2P28 and AR4P15) were identified at the species level through phylogenetic analysis. The colonies of *Lasiodiplodia* spp. exhibited white aerial mycelium, which transformed into dark green, gray, and eventually black after seven days, with uniform coloration on both the upper and lower surfaces. The mycelium was septate, branched, and dense, with smooth edges. The conidia, initially hyaline and unicellular, became brown and unicellular over time, with a smooth, ellipsoidal shape. Stromata were observed on the stems of *Pinus taeda* (Figure 2-A to F). In contrast, colonies of *Pestalotiopsis* spp. (AR1P13, AR2P15, AR4P25, AR5P19, AR7P34, AR9P10, AR10P11, AR11P13) presented a lobed edge with white to pale honey-yellow mycelium on the front, and the reverse side also pale honey-yellow, showing intense black punctuations due to sporulation. These colonies grew large, with a diameter greater than 70 mm after seven days, displaying an intense sporulation pattern (Figure 2-G to K). The conidia of *Pestalotiopsis* spp. were multinucleate, with dark septa, and had 4-5 cells. The apical and basal cells were hyaline, while the middle cells ranged from brown to honey-yellow. *Coniella* colonies (AR3P21, AR3P13, AR4P23, AR4P17) were dense, with white mycelium turning yellowish with age, exhibiting a more uniform texture and edge. The conidia of *Coniella* spp. were hyaline, unicellular, and oval to cylindrical in shape, without septation (Figure 2 L to P).



Figure 2 - Morphological characteristics observed of *Botryosphaeria*, *Pestalotiopsis* spp., and *Coniella* spp. in this study.



Source: The authors, 2021.

The length of the conidia of *Lasiodiplodia* spp. ranged from 8-15 μm , with a width of 4-7 μm , and the L/W ratio was between 1.20 to 1.80 μm (Table 3). These conidia were initially hyaline, unicellular, and ellipsoidal, becoming brown over time. In contrast, *Pestalotiopsis* spp. conidia ranged from 16-38 μm in length and 2-9 μm in width, with 4-5 cells. The apical and basal cells were hyaline, while the three median cells were brownish, with a more intense color in the central cells. The conidia of *Coniella* spp. were hyaline, unicellular, oval to cylindrical in shape, and lacked septa, ranging from 8-12 μm in length and 4-6 μm in width. In Table 3, it is also possible to observe additional characteristics of the isolates. A species of each genus was used for comparison: *Lasiodiplodia theobromae* (Phillips *et al.*, 2013), *Neopestalotiopsis surinamensis* (Maharachchikumbura *et al.*, 2014), and *Coniella fragariae* Oudemans (Alvarez *et al.*, 2016).



Table 3. Micromorphological characterization data of conidia from fungal specimens isolated from *Eucalyptus urophylla*, clone I144 and of type or representative species of each genus.

<i>Lasiodiplodia</i>					
Fungi	NC	Length (µm)		Width (µm)	L/W Ratio
<i>Lasiodiplodia theobromae</i>	2	av>25		av<16	av<2,0
AR2P28	2	23.46-26.30 (av=25.08; sd=0.98; mse=0.31)		11.58-13.17 (av=12.33; sd=0.49; mse=0.15)	1.90-2.21 (av=2.04; sd=0.10; mse=0.04)
AR3P13	2	22.27-27.36 (av=24.47; sd=1.73; mse=0.55)		10.27-13.71 (av=12.47; sd=1.12; mse=0.35)	1.65-2.31; (av=2.00; sd=0.26; mse=0.08)
AR3P21	2	20.15-27.03 (av=23.88; sd=2.12; mse=0.67)		11.88-14.06 (av=12.91; sd=0.67; mse=0.21)	1.68-2.01 (av=1.85; sd=0.10; sd=0.03)
AR4P15	2	22.62-29.89 (av=25.53; sd=2.15; mse=0.68)		10.22-14.23 (av=12.18; sd=1.16; mse=0.37)	1.72-2.56 (av=2.11; sd=0.24; mse=0.08)
AR4P23	2	19.83-29.47 (av=23.89; sd=3.05; mse=0.96)		11.52-14.24 (av=12.93; sd=0.88; mse=0.28)	1.72-2.56 (av=1.86; sd=0.34; mse=0.11)
<i>Coniella</i>					
Fungi	NC	Length (µm)		Width (µm)	L/W Ratio
<i>Coniella fragariae</i>	1	7,0-12,5		4-(6-8)-10	av=1,4
AR3P10	1	6.22-8.33 (av=7.24; sd=0.54; mse=0.10)		5.19-7.45 (av=6.31; sd=0.61; mse=0.11)	1.11-1.20 (av=1.15; sd=0.04; mse=0.01)
AR3P28	1	6.15-9.20 (av=7.79; sd=0.74; mse=0.13)		5.35-8.27 (x̄=6.98; dp=0.63; ep=0.12)	1.08-1.15 (x̄=1.12; dp=0.02; ep=0.01)
AR4P24	1	5.40-7.6 (av=6.60; sd=0.58; mse=0.11)		4.02-7.11 (av=5.79; sd=0.75; mse=0.14)	1.07-1.34 (av=1.15; sd=0.06; mse=0.01)
AR4P29	1	6.36-9.35 (av=7.54; sd=0.66; mse=0.12)		5.46-7.55 (av=6.50; sd=0.60; mse=0.11)	1.11-1.24 (av=1.16; sd=0.02; mse=0.1)
<i>Neopestalotiopsis</i>					
Fungi	NC	AA	BA	Length (µm)	Width (µm)
<i>Neopestalotiopsis surinamensis</i>	-	2-3	1	(23-) 24-28 (-29) (av=27.7; sd=1.0)	(7.0-) 7.5-9.0 (-9.5) (av=8.1; sd=0.4)
AR1P17	5	2-4	1	16.61-24.94 (av=20.41; sd=2.14; mse=0.39)	2.40-9.15 (av=6.71; sd= 1.30; mse=0.24)
AR1P22	5	2-3	1	14.57-37.95 (av=22.14; sd=4.72; mse= 0.86)	4.86-8.82 (av=5.68; sd=0.50; mse= 0.09)
AR2P14	5	2-3	1	16.91-28.07 (av=22.17; sd=2.79; mse= 0.51)	4.55-7.62 (av=6.05; sd=0.74; mse= 0.14)
AR2P29	5	2-3	1	16.09-25.87 (av=22.19; sd=2.42; mse=0.45)	5.83-8.24 (av=6.88; sd=0.71; mse= 0.13)
AR3P15	5	2-3	1	16.28-25.69 (av=20.15; sd=2.12; mse=0.39)	4.40-6.13 (av=5.26; sd=0.50; mse=0.09)
AR3P25	5	2-3	1	18.82-25.38 (av=21.12; sd=1.58; mse=0.29)	4.13-5.88 (av=5.03; sd=0.46; mse=0.08)
AR4P19	5	2-3	1	15.66-22.10 (av=18.64; sd=1.33; mse=0.24)	3.52-6.61 (av=4.77; sd=0.68; mse= 0.12)
AR4P21	5	2-3	1	17.25-24.87 (av=21.86; sd=1.71; mse=0.31)	5.05-7.23 (av=6.03; sd=0.60; mse=0.11)

Number of measured conidia (n) = 30 for *Pestalotiopsis* and *Coniella*, and (n) = 10 for *Lasiodiplodia*. AA = Apical Appendix; BA = Baseline Appendix; NC = Number of conidia cells; L/W ratio = Length/width ratio; av = average; sd = standard deviation and mse = mean standard error.

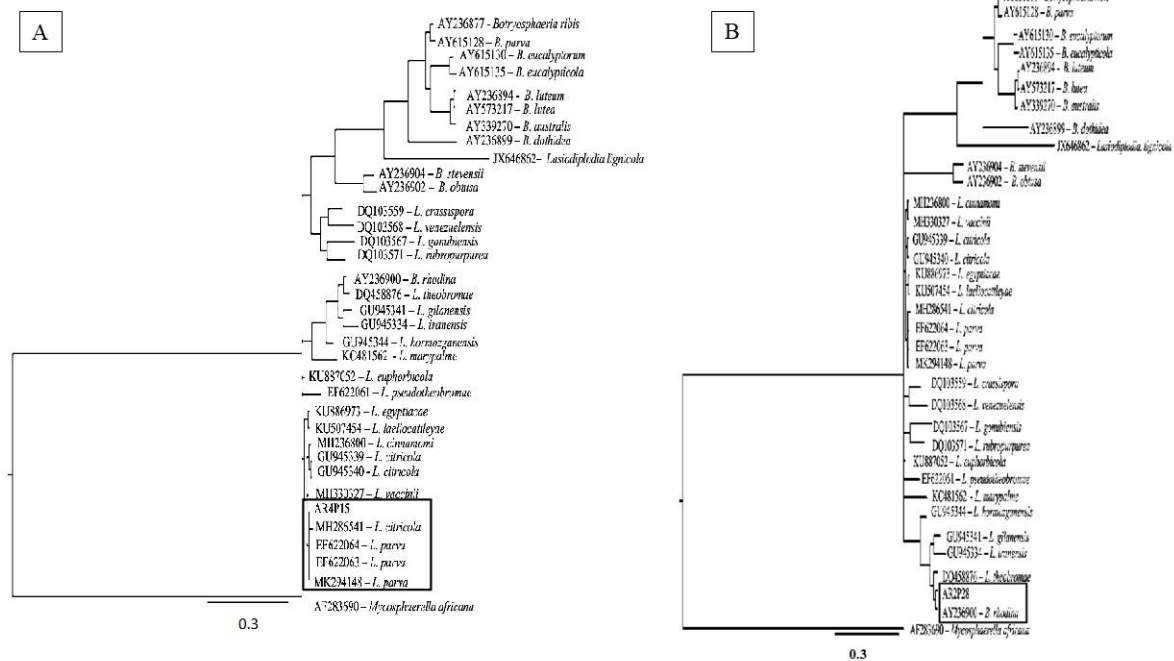
Source: The authors, 2021.

The TEF1-α sequences were about 250 bp in size, the ITS rDNA sequences were



approximately 490 bp in size, and the criterion of 100% homology to any taxon included in the analysis was considered for species identification. Phylogenetic analyzes with non-concatenated *tef1* or ITS genomic sequences were used to identify strains of putative *Lasiodiplodia* spp. and from *Pestalotiopsis* spp. The strain *Lasiodiplodia* spp. AR2P28 showed 100% homology to *B. rhodina* AY236900 (Figure 3-A) by TEF1- α sequence analysis and the strain *Lasiodiplodia* spp. AR4P15 showed 100% homology with *Lasiodiplodia citricola* GU945353 (Figure 3-B).

Figure 3. Phylogenetic tree of the AR4P15 and AR2P28 isolateS clustering through Bayesian inference of TEF1 sequences using *Botryosphaeria* and *Lasiodiplodia* species and *Mycosphaerella africana* as the outgroup.

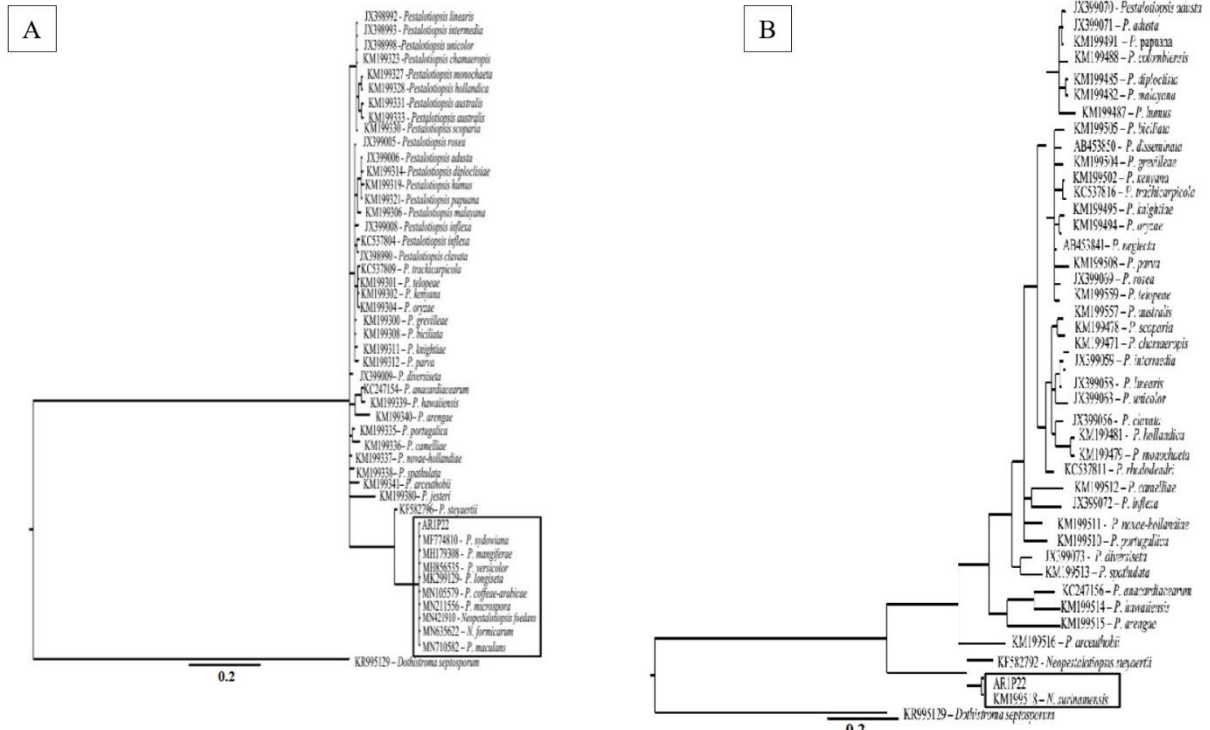


Source: The authors, 2021.

The strain *Pestalotiopsis* spp. (AR1P22) showed 100% homology with *Neopestalotiopsis surinamensis* KM199518 by TEF1- α sequence analysis (Figure 4-A), while for the ITS region, it aligned with species of *Pestalotiopsis* (Figure 4-B).



Figure 4. Phylogenetic tree of the AR1P22 isolate clustering through Bayesian inference of TEF1 and ITS sequences using *Pestalotiopsis* spp. and *Neopestalotiopsis* spp. and *Dothistroma septosporum* as the outgroup.



Source: The authors, 2021.

The fungi selected in the population of diseased plant isolates were identified as *Lasiodiplodia* spp., *Pestalotiopsis* spp., and *Coniella* spp. using macro- and micromorphological characterization, followed by phenotypic distance matrix calculation and cluster analysis (UPGMA). Chen *et al.* (2015) reported that the clear identification of *Lasiodiplodia* species was not possible using conidia and colony morphology alone due to significant character overlap between species, which was also observed in this study. However, the identification of *Eucalyptus* specimens in the genus *Lasiodiplodia*. These findings are supported by previous studies (Phillips *et al.*, 2013; Chen *et al.*, 2014; Slippers *et al.*, 2014).

Maharachchikumbura *et al.* (2011) emphasized that conidia characteristics and the pigmentation of median cells are critical in differentiating *Pestalotiopsis* isolates. However, there is significant phenotypic overlap, making it difficult to separate morphologically misclassified taxa (Hu *et al.*, 2007; Tejesvi *et al.*, 2009). Maharachchikumbura *et al.* (2013; 2014) revealed that species with similar conidia dimensions did not cluster in molecular analyses, demonstrating that classifying *Pestalotiopsis* species based solely on conidia length and width is inaccurate. Instead, a combination of morphological and molecular characterization is required.



Abdollahzadeh *et al.* (2010) highlighted that phylogenetics plays a crucial role in differentiating *Lasiodiplodia* species. In this study, this was confirmed, as morphological characterization allowed only genus-level identification, while molecular analysis successfully classified species. The TEF1- α sequence efficiently identified isolate AR2P28 as *Lasiodiplodia theobromae*, while the ITS sequence confirmed AR4P15 as *Lasiodiplodia citricola*.

Alves *et al.* (2008) used ITS and TEF1- α with morphological data to characterize isolates initially identified as *L. theobromae*, revealing that *L. theobromae* is a species complex. They described new species, *L. pseudotheobromae* and *L. parva*, while Abdollahzadeh *et al.* (2010) identified four additional species. They also noted that species within the *Lasiodiplodia* complex cannot be distinguished solely by ITS sequences, and phylogenetic classification is more effective using TEF1- α .

The genus *Pestalotiopsis* is reported as the causal agent of leaf spots and stem lesions in *Eucalyptus* cuttings and mini-cuttings during the nursery phase (Alfenas *et al.*, 2004). It is also linked to drought-induced apex lesions in *Eucalyptus* in the Vale do Rio Doce (Ferreira & Milani, 2002). Santos *et al.* (2020) confirmed the presence of at least three *Neopestalotiopsis* species (a genus derived from *Pestalotiopsis*) as etiological agents of leaf spots and stem rot in *Eucalyptus* cuttings in Brazil. While *Pestalotiopsis* spp. have not been reported as primary pathogens of *Eucalyptus* cankers, they are recognized as secondary and opportunistic pathogens in SPEVRD and Botryosphaeria canker (Ferreira & Milani, 2002; Alfenas *et al.*, 2004). Additionally, *Pestalotiopsis* spp. have been identified as contributors to white rot in *Eucalyptus* forests (Alonso *et al.*, 2007).

The genus *Lasiodiplodia*, identified in this study, along with *Botryosphaeria* spp., has been reported as a pathogen of *Eucalyptus* in several countries. Slippers *et al.* (2009) documented a high diversity of Botryosphaeriaceae species infecting *Eucalyptus* spp. *L. theobromae* has been found on hundreds of host plants, including *Eucalyptus*, and has been reported in multiple countries, including those in South America (Roux *et al.*, 2001; Burgess *et al.*, 2006). It is considered one of the most aggressive and harmful Botryosphaeriaceae species affecting *Eucalyptus* (Pavlic *et al.*, 2008). According to the International Code of Nomenclature for Algae, Fungi, and Plants, *L. theobromae* is the only currently valid taxon, with no recognized connection to a sexual phase.



3.3 EVALUATION OF THE SPATIAL PATTERN OF THE DISEASE

In this study, the Dispersion Index, DI, values of areas 1, 3, and 4 were statistically higher than 1 in both quadrats, indicating that the disease presents an aggregated spatial pattern in these areas, except in P2 of area 1 in the quadrat 3x2. In contrast, area 2 showed a DI value not significantly different from 1, indicating a random disease pattern in both quadrats, except for P1 in the 3x2 quadrat. The χ^2 and d statistics corroborated the conclusions of the spatial patterns of the disease population from the Dispersion Index, DI, in all plots of areas 3 and 4 for both quadrat sizes and P1 of areas 1 and P2 of area 2. P2 in area 1 and P1 in area 2 showed different spatial patterns for each quadrat size (Table 4).

Table 4. Incidence (I), dispersion index (DI), chi-square tests, and spatial dispersion pattern per plot of diseased plants of *Eucalyptus urophylla*, clone I144, in areas Ar1, Ar2, Ar3, and Ar4.

Quadrats/ Areas	I ⁽¹⁾	DI ⁽²⁾	χ^2 obs ⁽³⁾	χ^2 calc ⁽⁴⁾	SP ⁽⁵⁾	I ⁽¹⁾	DI ⁽²⁾	χ^2 obs ⁽³⁾	χ^2 calc ⁽⁴⁾	PE ⁽⁵⁾
	Q 2x2	Q 2x2	Q 2x2	Q 2x2	Q 2x2	Q 3x2	Q 3x2	Q 3x2	Q 3x2	Q 3x2
Ar1.P1	31.5 2	2.36 ^{n.s.}	269.35 ^{n.s.}	139.64	a	32.44	3.28 ^{n.s.}	243.17 ^{n.s.}	94.80	a
Ar1.P2	98.7 5	1.31 ^{n.s.}	155.95 ^{n.s.}	145.18	a	93.54	0.73*	57.90*	100.46	r
av. ^{n.t.}	65.1 4	1.84	212.65	142.41		62.99	2.01	150.54	97.63	
Ar2.P1	26.6 7	1.22*	145.05*	145.18	r	26.25	1.31 ^{n.s.}	104.64 ^{n.s.}	100.46	a
Ar2.P2	41.2 5	0.88*	104.50*	145.18	r	40.40	0.93*	73.05*	100.50	r
av. ^{n.t.}	33.9 6	1.05	124.78	145.18		33.325	1.12	88.85	100.48	
Ar3.P1	82.1 0	1.36 ^{n.s.}	160.70 ^{n.s.}	144.10	a	81.84	1.90 ^{n.s.}	146.19 ^{n.s.}	98.20	a
Ar3.P2	78.6 0	1.74 ^{n.s.}	190.00 ^{n.s.}	134.10	a	78.60	2.30 ^{n.s.}	167.50 ^{n.s.}	93.66	a
av. ^{n.t.}	80.3 5	1.55	175.35	139.1		80.22	2.10	156.85	95.93	
Ar4.P1	86.3 2	1.47 ^{n.s.}	160.20 ^{n.s.}	144.10	a	86.30	1.57 ^{n.s.}	120.69 ^{n.s.}	98.20	a
Ar4.P2	86.5 4	1.48 ^{n.s.}	161.53 ^{n.s.}	142.96	a	86.32	1.97 ^{n.s.}	151.82 ^{n.s.}	98.20	a
av. ^{n.t.}	86.4 3	1.48	160.87	143.53		86.31	1.77	136.26	98.2	

I⁽¹⁾ Botryosphaeria Canker Incidence in whole quadrats, in (%); ⁽²⁾ DI= Dispersion Index; (^{n.s.}) = not significant and (^{*}) = significant at 5% (P>0.05) probability by the chi-square test (χ^2); av.^(n.t.) = average untested value; ⁽³⁾ χ^2 obs = observed chi-square calculated = χ^2 obs(c); (^{n.s.}) = non-significant test and (^{*}) = 5% significant (P>0.05) by the chi-square test, (χ^2); ⁽⁴⁾ χ^2 calc = $0.5 * [1.645 + (2 * (N-1) - 1)^{0.5}]^2$; ⁽⁵⁾ SP = spatial pattern; a=aggregate; r=random.

Source: Elaborated by the authors.



It was found that the average number of observed runs (R) in the planting lines for areas 1, 2, and 4 were lower than the average number of expected runs $E(R)$ and that the standardized values (Z_R) were ≥ -1.64 . Therefore, H_0 was accepted at 5% probability for these three areas, and the dispersion pattern or the disease's spatial distribution in the planting lines was random. Regarding area 3, it was found that the number of runs observed (R) was lower than the number of runs expected $E(R)$, and $Z_R < -1.64$. H_0 of the random spatial pattern was rejected, and H_a of the aggregated spatial pattern was accepted in the planting lines (Table 5). The run test showed a predominance of the random spatial pattern in areas 1, 2, and 4, with 80%, 95%, and 71.67% of the lines with this spatial pattern, respectively. In area 3, 75.71% of the planting lines showed an aggregated spatial pattern.

Table 5. Run analysis parameters by plotting areas Ar1, Ar2, Ar3, and Ar4 for data on diseased and healthy plants of *Eucalyptus urophylla* clone I144, in the planting lines.

Area	Plot	Number of lines	R	$E(R)$	$\sigma^2(R)$	$\sigma(R)$	m	N	Z_R	SP
Ar1	1	15	7	10	2.95	1.47	11	33	-0.91*	r
	2	20	2	2	0.04	0.10	25	25	0.50*	r
	av ^{n.t.}	17.5	4.28	5.77	1.49	0.78	17.76	29.20	-0.20	
Ar2	1	20	9	9	2.86	1.61	7	25	0.10*	r
	2	20	11	12	4.55	2.11	10	25	-0.15*	r
	av ^{n.t.}	20	9.93	10.62	3.70	1.86	8.55	25.00	-0.02	
Ar3	1	7	15	20	5.77	2.11	59	71	-1.42*	r
	2	5	21	32	9.97	2.98	80	100	-3.25 ^{n.s.}	a
	av ^{n.t.}	6	18.14	25.86	7.87	2.55	69.64	85.71	-2.33	
Ar4	1	6	14	16	4.52	1.57	73	83	-0.03*	r
	2	10	7	11	3.11	1.31	44	50	-0.84*	r
	av ^{n.t.}	8	10.43	13.57	3.82	1.44	58.08	66.67	-0.44	

Where: R = runs; $E(R)$ = expected runs; $\sigma^2(R)$ = variance; $\sigma(R)$ = standard deviation N = number of plants; m = number of diseased plants; Z_R = standardized value; SP = spatial pattern; a = aggregate; r = random; av^(n.t.) = average untested value; (*) = significant at 5% probability, H_0 is accepted; (n.s.) = not significant at 5% probability, rejects H_0 .

Source: Elaborated by the authors.

By the doublet test, it was found that the average number of doublets observed (D) in the planting lines for areas 1 and 2 were more significant than the average number of doublets expected $E(D)$, however the values (Z_D) < 1.64 , (Table 6). H_0 : random spatial pattern (random) was accepted for areas 1 and 2, and H_a a was rejected ($p=0.05$). As for areas 3 and 4, the numbers of doublets observed (D) were greater than those expected $E(D)$ and Z_D values > 1.64 (Table 6). H_0 : random spatial pattern (random) was rejected, and H_a : aggregated spatial pattern a ($p=0.05$) was accepted.



Table 6. Parameters of *doublet* analysis by plotting areas Ar1, Ar2, Ar3, and Ar4 for data on diseased and healthy plants of *Eucalyptus urophylla*, clone I144, in the planting lines.

Area	Plot	Number of lines	<i>D</i>	<i>E(D)</i>	$\sigma^2(D)$	$\sigma(D)$	<i>m</i>	<i>N</i>	<i>Z_D</i>	SP
Ar1	1	15.0	7	6	6.04	2.05	11	33	0.96*	r
	2	20.0	23	23	0.03	0.09	25	25	1.06*	r
	av. ^{n.t}	17.5	15.4	14.7	3.04	1.07	17.8	29.2	1.01	
Ar2	1	20.0	2	2	0.73	0.80	7	25	0.88*	r
	2	20.0	5	5	1.21	1.08	10	25	0.77*	r
	av. ^{n.t}	20.0	3.7	3.4	0.97	0.94	8.6	25.0	0.82	
Ar3	1	7.0	51	49	1.58	1.13	59	71	2.24 ^{n.s.}	a
	2	5.0	69	64	2.66	1.55	80	100	3.56 ^{n.s.}	a
	av. ^{n.t}	6.0	60.1	56.4	2.12	1.34	69.6	85.7	2.90	
Ar4	1	6.0	66	64	1.22	0.85	73	83	1.99 ^{n.s.}	a
	2	10.0	40	38	0.89	0.72	44	50	1.99 ^{n.s.}	a
	av. ^{n.t}	8.0	52.6	50.9	1.05	0.78	58.1	66.7	1.99	

Where: *D* = doublets; *E(D)* = expected doublets; $\sigma^2(D)$ = variance; $\sigma(D)$ = standard deviation; *m* = number of diseased plants; *N* = total number of plants; *Z_R* = standardized value; SP = spatial pattern; a = aggregate; r = random; av.^(n.t) - average untested value; (*) = significant at 5% probability, H0 is accepted; (n.s.) = not significant at 5% probability, rejects H0

Source: Elaborated by the authors.

By the priority rule, areas 1, 2, and 4 were considered with random spatial patterns in the lines, and area 3 with aggregated spatial patterns, by both tests. The frequency of spatial pattern lines per area by run analysis ranged from 24.29% to 95.00% of lines with random spatial pattern and by doublet analysis from 24.29% to 91.67% for this pattern. Area 3 presented 75.71% of the lines with an aggregated spatial pattern for both tests.

The analysis of the Dispersion Index (DI) shows that $DI < 1$ indicates regular distribution, $DI = 1$ random distribution, and $DI > 1$ aggregated distribution (Campbell & Madden, 1990; Bergamin Filho *et al.*, 2004). In this study, DI values of areas 1, 3, and 4 were higher than 1 in both quadrat sizes, indicating an aggregated spatial pattern of the disease, characteristic of overdispersion or contagious dispersion. In area 2 (ICLF system), DI values were not statistically different from 1, indicating a regular spatial distribution of the disease, characteristic of a binomial distribution and regular dispersion.

The χ^2 and d statistics confirmed the spatial patterns from the Dispersion Index. In areas 3 and 4, for both quadrat sizes, and P1 of area 1 and P2 of area 2, patterns were consistent. P2 of area 1 and P1 of area 2 showed different spatial patterns for each quadrat size. The aggregated spatial pattern indicates the presence of a biotic agent causing the disease, with high infective power in susceptible plants, mainly along the planting line (Tumura *et al.*, 2012). This results in small-scale aggregation, overdispersion, and heterogeneity in space occupation.



Agreement was found for areas 1, 2, and 3 by comparing run and doublet methods of spatial evaluation. However, for area 4, there was a divergence between spatial patterns in the lines. Madden *et al.* (1982) consider runs more appropriate than doublets for determining the randomness of diseased plants. Masson (2009) emphasized that these tests are valuable epidemiologically, helping to infer pathogen dispersion efficiency, its infective potential, and aggregation patterns in the field. The regular dispersion of the disease in area 3 indicates homogeneous probability of infection and disease development in space occupation.

3.4 ANALYSIS OF THE DYNAMICS AND STRUCTURE OF FOCUS

By ADSF, the disease had a higher incidence in the ICLF system than in the PS system, with differences of 23.6% to 155%. Incidence ranged from 34.20% to 87.20%, with few foci, mostly compact, and a large number of diseased plants, especially in areas 3 and 4 of the ICLF system.

The number of unitary foci (NUF) was low, with 2, 10, 1, and 0 foci for areas 1, 2, 3, and 4, respectively. Non-unitary foci (NFNU) were 6, 17, 2, and 2 for the areas. In area 1, the average number of foci was 7 with 255 plants per focus (ANPF). Area 2 had 26 foci with 11 plants per focus, and areas 3 and 4 had 3 and 2 foci, respectively, with 306 and 327 plants per focus. IFF and IFFNU were < 1 in most plots, indicating foci aligned with planting lines. In plot 1 of area 2, $IFF > 1$ and $IFNUF > 1$, indicating greater focus length. ICF values ranged from 0.5 to 1.0, and ICNUF values from 0.6 to 1.0, showing foci compactness (Table 7).

Table 7. Incidence (I) and parameters of the analysis of the dynamics and structure of foci (ADSF) by plotting areas Ar1, Ar2, Ar3, and Ar4 for diseased and healthy plants *Eucalyptus urophylla*, clone I144.

Area	Plot	I ⁽¹⁾	NDP	NF	NUF	ANPF	IFF	ICF	IFNUF	ICNUF
Ar1	1	32.60	163	13	3	16.30	0.8	0.7	0.7	0.6
	2	98.80	494	1	0	494.00	0.8	1.0	0.8	1.0
	av.	65.70	329	7.00	1.50	255.15	0.8	0.9	0.8	0.8
Ar2	1	26.80	134	31	11	6.15	1.2	0.8	1.3	0.7
	2	41.60	208	21	8	15.38	0.8	0.8	0.7	0.7
	av.	34.20	171	26.00	9.50	10.77	1.0	0.80	1.0	0.7
Ar3	1	83.00	415	1	0	415.00	0.1	0.6	0.1	0.6
	2	79.40	397	4	2	197.50	0.5	0.5	0.1	0.7
	av.	81.20	406	2.50	1.00	306.25	0.3	0.6	0.1	0.7
Ar4	1	87.20	436	1	0	436.00	0.1	0.7	0.1	0.7
	2	87.20	435	2	0	218.00	0.1	0.8	0.1	0.8
	av.	87.20	436	1.50	0.00	327.00	0.1	0.8	0.1	0.8



Where: $I^{(1)}$ = incidence of Botryosphaeria Canker in whole plots of 500 plants, in (%); NDP- Number of diseased plants; NF = number of focus per plot; NUF = number of unitary foci; ANPF = average number of plants per non-unitary foci; IFF = average index of shape of foci and ICF= average index of compaction of foci, IFNUF = average index of the form of non-unitary foci and ICNUF = average index of compaction of non-unitary foci.

Source: Elaborated by the authors.

There was a negative Pearson correlation between incidence I and number of foci (NF), $r = -0.9125266$, significant at 95% probability ($t = -5.4649$, p -value = 0.001565, $df = 6$), with a confidence interval from -0.9842771 to -0.5822768. In areas with incidence $> 65\%$ (areas 1, 3, and 4), NF was ≤ 7 , while area 2, with lower incidence (34.20%), had the largest number of foci (NF = 26). These results align with Jesus Junior and Bassanezi (2004), who found maximum foci in citrus stands at 18% incidence, decreasing with higher incidence. When studying unitary foci, they found the maximum at 13%, decreasing with incidence increase. Based on IFF and IFNUF, the disease showed predominant spatial dispersion along planting lines. Foci were compact, indicating aggregation of diseased plants. Similar results were observed in *Eucalyptus* studies (Souza, 2007; Tumura *et al.*, 2012). Integrated agricultural systems are expanding in Brazil, reducing disease intensity (Roese *et al.*, 2020).

4 CONCLUSIONS

It is concluded that *Eucalyptus urophylla*, clone I144, disease, is characterized by lesions with elongated cankers in high positions on the stem, die-back, stem bifurcation with signs of loss of apical dominance, tortuosity in the stem or trunk, dwarfism, and the frequent presence of kino in the lesions, in a pure stand system, PS, or ICLF system with *Urochloa brizantha* in the studied sites. It is of biotic origin, caused by the pathogen *Lasiodiplodia theobromae* and called Botryosphaeria Canker. However, *Lasiodiplodia citricola* was identified in a sample from area IV, indicating possible species diversity of *Lasiodiplodia* in Botryosphaeria Canker in Brazil. *Neopestalotiopsis surinamensis* was identified in a sample from area 1.

According to the Dispersion Index, DI, the disease presents an aggregated spatial pattern in areas 1, 3, and 4, except in P2 of area 1, for a 3x2 quadrat, and a random spatial pattern in area 2, except in P1 of the 3x2 quadrat. In the direction of the lines, the disease presented a random spatial pattern in areas 1, 2 and an aggregated spatial pattern in areas 3 and 4 by the *doublet* test priority criterion.

By ADSF concluded that the disease had a higher incidence in the ICLF system than in



the PS system. The disease occurred with an high incidence in both of them with a low number of foci, mostly compact foci, and a large number of diseased plants per focus, mainly in areas 3 and 4 in the ICLF system.

ACKNOWLEDGEMENTS

To Dr. Celso Garcia Auer, Dr. Rivalalve Coelho Gonçalves, Professors Dr. Nei Sebastião Braga and Dr. Waldir Cintra de Jesus Junior for their support in the method, writing, and revision of the text. To Professor Dr. Anete Pereira de Souza, Patrícia Zambon, and other colleagues from the Genotyping and Sequencing Laboratory at the State University of Campinas, Campinas-SP, for the sequencing work. To CAPES for granting scholarships and financial support to carry out this work.



REFERENCES

- ABDOLLAHZADEH, J.; JAVADI, A.; MOHAMMADI GOLTAPEH, E.; ZARE, R.; PHILLIPS, A. J. L. Phylogeny and morphology of four new species of *Lasiodiplodia* from Iran. **Persoonia**, v. 25, p. 1-10, 2010.
- ALFENAS, A. C.; ZAUZA, E. A. V.; MAFIA, R. G.; ASSIS, T. F. **Clonagem e doenças do eucalipto**. Viçosa: Editora UFV, 2004. 442 p.
- ALFENAS, A. C.; FERREIRA, F. A.; MAFIA, R. G.; GONÇALVES, R. C. Isolamento de fungos fitopatogênicos. In: ALFENAS, A. C.; MAFIA, R. G. (Org.). **Métodos em Fitopatologia**. Viçosa: Editora UFV, 2007. p. 53-90.
- ALONSO, S. K.; SILVA, A. G.; KASUYA, M. C. M.; BARROS, N. F.; CAVALLAZZI, J. R. P.; BETTUCCI, L.; LUPO, L.; ALFENAS, A. C. Isolamento e seleção de fungos causadores da podridão-branca da madeira em florestas de *Eucalyptus spp.* com potencial de degradação de cepas e raízes. **Revista Árvore**, v. 31, p. 145-155, 2007.
- ALTEKAR, G.; DWARKADAS, S.; HUELSENBECK, J.; RONQUIST, F. Parallel Metropolis Coupled Markov Chain Monte Carlo for Bayesian phylogenetic inference. **Bioinformatics**, v. 20, p. 407-415, 2004.
- ALVAREZ, L. V.; GROENEWALD, J. Z.; CROUS, P. W. Revising the *Schizoparmaceae*: *Coniella* and its synonyms *Pilidiella* and *Schizoparme*. **Studies in Mycology**, v. 85, p. 1-34, 2016.
- ALVES, A.; CROUS, P. W.; CORREIA, A.; PHILLIPS, A. J. L. Morphological and molecular data reveal cryptic speciation in *Lasiodiplodia theobromae*. **Fungal Diversity**, v. 28, p. 1-13, 2008.
- BERGAMIN FILHO, A.; HAU, B.; AMORIM, L.; JESUS JUNIOR, W. C. de. Análise espacial de epidemias. In: VALE, F. X. R. do; JESUS JUNIOR, W. C. de; ZAMBOLIM, L. (Org.). **Epidemiologia aplicada ao manejo de doenças de plantas**. Belo Horizonte: Editora Folha de Viçosa Ltda, 2004. p. 195-240.
- BHERING, L. L. **Rbio: a tool for biometric and statistical analysis using the R platform**. **Crop Breeding and Applied Biotechnology**, v. 17, p. 187-190, 2017.
- BURGESS, T. I.; BARBER, P. A.; MOHALI, S.; PEGG, G.; DE BEER, W.; WINGFIELD, M. J. Three new *Lasiodiplodia* spp. from the tropics, recognised based on DNA sequence comparisons and morphology. **Mycologia**, v. 98, p. 423-435, 2006.
- CAMPBELL, C. L.; MADDEN, L. V. **Introduction to plant disease epidemiology**. New York: John Wiley & Sons, 1990. 532 p.
- CARBONE, I. A.; KOHN, L. M. A method for designing primer sets for the speciation studies in filamentous ascomycetes. **Mycologia**, v. 91, p. 553-556, 1999.



CHEN, S.; MORGAN, D. P.; HASEY, J. K.; ANDERSON, K.; MICHAILIDES, T. J. Phylogeny, morphology, distribution, and pathogenicity of *Botryosphaeriaceae* and *Diaporthaceae* from English walnut in California. **Plant Disease**, v. 98, p. 636-652, 2014.

CHEN, S.; LI, G.; LIU, F.; MICHAILIDES, T. J. Novel species of *Botryosphaeriaceae* associated with shoot blight of pistachio. **Mycologia**, v. 107, p. 780-792, 2015.

DOYLE, J. J.; DOYLE, J. L. A rapid DNA isolation procedure for small quantities of fresh leaf tissue. **Phytochemical Bulletin**, v. 19, p. 11-15, 1987.

ELLIOTT, J. M. **Some methods for the statistical analysis of samples of benthic invertebrates: Scientific Publication 25**. Ambleside: Freshwater Biological Association, 1993. 159 p.

FERREIRA, F. A.; MILANI, D. **Diagnose visual e controle das doenças abióticas e bióticas do eucalipto no Brasil**. Mogi Guaçu: International Paper, 2002. 98 p.

HALL, T. A. BioEdit: a user-friendly biological sequence alignment editor and analysis program for Windows 95/98/NT. **Nucleic Acids Symposium Series**, v. 41, p. 95-98, 1999.

HU, H.; JEEWON, R.; ZHOU, D.; ZHOU, T.; HYDE, K. D. Phylogenetic diversity of endophytic *Pestalotiopsis* species in *Pinus armandii* and *Ribes* spp.: evidence from rDNA and beta-tubulin gene phylogenies. **Fungal Diversity**, v. 24, p. 1-22, 2007.

IBA. *Relatório anual 2020*. Disponível em:
<https://iba.org/datafiles/publicacoes/relatorios/ibarelatorioanual2019.pdf>. Acesso em: 11 maio 2020.

JESUS JUNIOR, W. C. de; BASSANEZI, R. B. Análise da dinâmica e estrutura de focos da morte súbita dos citros. **Fitopatologia Brasileira**, v. 29, p. 399-405, 2004.

KUMAR, S.; STECHER, G.; LI, M.; KNYAZ, C.; TAMURA, K. MEGA X: molecular evolutionary genetics analysis across computing platforms. **Molecular Biology and Evolution**, v. 6, p. 1547-1549, 2018.

MAHARACHCHIKUMBURA, S. N. S.; GUO, L. D.; CHUKEATIROTE, E.; BAHKALI, A. H.; HYDE, K. D. *Pestalotiopsis*: morphology, phylogeny, biochemistry and diversity. **Fungal Diversity**, v. 50, p. 167-187, 2011.

MAHARACHCHIKUMBURA, S. N. S.; GUO, L. D.; CHUKEATIROTE, E.; MCKENZIE, E. H. C.; HYDE, K. D. A destructive new disease of *Syzygium samarangense* in Thailand caused by the new species *Pestalotiopsis samarangensis*. **Tropical Plant Pathology**, v. 38, p. 227-235, 2013.

MAHARACHCHIKUMBURA, S. N. S.; HYDE, K. D.; GROENEWALD, J. Z.; XU, J.; CROUS, P. W. *Pestalotiopsis* revisited. **Studies in Mycology**, v. 79, p. 121-186, 2014.



MASSON, M. V. **Ferrugem do eucalipto: planejamento evasivo, estimativa de dano e análise da viabilidade do controle químico**. 2009. 174 p. Tese (Doutorado) – Faculdade de Ciências Agrônômicas, Universidade Estadual Paulista, Botucatu, São Paulo, Brasil.

NELSON, S. C. A simple analysis of disease foci. **Phytopathology**, v. 86, p. 332-339, 1996.

NYLANDER, J. A. A. **MrModeltest v2**. Program distributed by the author. Sweden: Dept. Systematic Zoology, Evolutionary Biology Centre of Uppsala University, 2004. Disponível em: <https://github.com/MrModeltest2/releases>. Acesso em: 15 abr. 2020.

OKSANEN, J. **Vegan: Community Ecology Package**. R package version 2.5-6, 2019. Disponível em: <https://CRAN.R-project.org/package=vegan>. Acesso em: 10 ago. 2019.

PAVLIC, D.; WINGFIELD, M. J.; BARBER, P.; SLIPPERS, B.; HARDY, G. E. St. J.; BURGESS, T. I. Seven new species of the *Botryosphaeriaceae* from baobab and other native trees in Western Australia. **Mycologia**, v. 100, p. 851-866, 2008.

PHILLIPS, A. J. L.; ALVES, A.; ABDOLLAHZADEH, J.; SLIPPERS, B.; WINGFIELD, M. J.; GROENEWALD, J. Z.; CROUS, P. W. The *Botryosphaeriaceae*: genera and species known from culture. **Studies in Mycology**, v. 76, p. 51-167, 2013.

RAMBAUT, A. **Figtree v. 1.2.2**. Computer program distributed by the author, 2009. Disponível em: <http://tree.bio.ed.ac.uk/software/figtree/>. Acesso em: 15 abr. 2020.

ROESE, A. D.; ZIELINSKI, E. C.; DE MIO, L. L. M. Plant diseases in afforested crop-livestock systems in Brazil. **Agricultural Systems**, v. 185, p. 1-13, 2020.

RONQUIST, F.; HEULSENBECK, J. P. MRBAYES 3: Bayesian phylogenetic inference under mixed models. **Bioinformatics**, v. 19, p. 1572-1574, 2003.

ROUX, J.; COUTINHO, T. A.; BYABASHAIJA, D. M.; WINGFIELD, M. J. Diseases of plantation *Eucalyptus* in Uganda. **South African Journal of Science**, v. 97, p. 16-18, 2001.

SLIPPERS, B.; BURGESS, T.; PAVLIC, D.; AHUMADA, R.; MALEME, H.; MOHALI, S.; RODAS, C.; WINGFIELD, M. J. A diverse assemblage of *Botryosphaeriaceae* infect *Eucalyptus* in native and non-native environments. **Journal of Forest Science**, v. 1, p. 101-110, 2009.

SLIPPERS, B.; ROUX, J.; WINGFIELD, M. J.; VAN DER WALT, F. J. J.; JAMI, F.; MEHL, J. W. M.; MARAIS, G. J. Confronting the constraints of morphological taxonomy in the *Botryosphaeriales*. **Persoonia**, v. 33, p. 155-168, 2014.

SANTOS, G. S.; MAFIA, R. G.; AGUIAR, A. M.; ZARPELON, T. G.; DAMACENA, M. B.; BARROS, A. F.; FERREIRA, M. A. Stem rot of *Eucalyptus* cuttings caused by *Neopestalotiopsis* spp. in Brazil. **Journal of Phytopathology**, v. 168, p. 311-321, 2020.

SOUZA, S. E. **Dinâmica espaço-temporal e danos do cancro basal em *Eucalyptus grandis***. 2007. 160 p. Tese (Doutorado) – Faculdade de Ciências Agrônômicas, Universidade Estadual Paulista, Botucatu, São Paulo, Brasil.



SOKAL, R. R.; MICHENER, C. D. A statistical method for evaluating systematic relationships. **The University of Kansas Scientific Bulletin**, v. 38, p. 1409-1438, 1958.

TEJESVI, M. V.; TAMHANKAR, S. A.; KINI, K. R.; RAO, V. S.; PRAKASH, H. S. Phylogenetic analysis of endophytic *Pestalotiopsis* species from ethnopharmacologically important medicinal trees. **Fungal Diversity**, v. 38, p. 167-183, 2009.

TUMURA, K. G.; PIERI, C.; FURTADO, E. L. Murcha por *Ceratocystis* em *Eucalyptus*: avaliação de resistência e análise epidemiológica. **Summa Phytopathologica**, v. 38, p. 54-60, 2012.

WINGFIELD, M. J.; SLIPPERS, B.; HURLEY, B. P.; COUTINHO, T. A.; WINGFIELD, B. D.; ROUX, J. *Eucalypt* pests and diseases, growing threats to plantation productivity. **Southern Forests**, v. 70, p. 139-144, 2008.